MVIRT – A Toolbox for Manifold-valued Image Restoration

Ronny Bergmann

Technische Universität Kaiserslautern

IEEE International Conference on Image Processing 2017

September 18, 2017,
Beijing, China.

supported by DAAD

Manifold-valued image processing

New data aquisition modalities $\Rightarrow$ non-Euclidean range of data

- **Interferrometric synthetic aperture radar (InSAR)**
- Surface normals
- Diffusion tensors in magnetic resonance imaging (DT-MRI)
- Electron backscattered diffraction (EBSD)
- Directional data: wind, flow, GPS,...

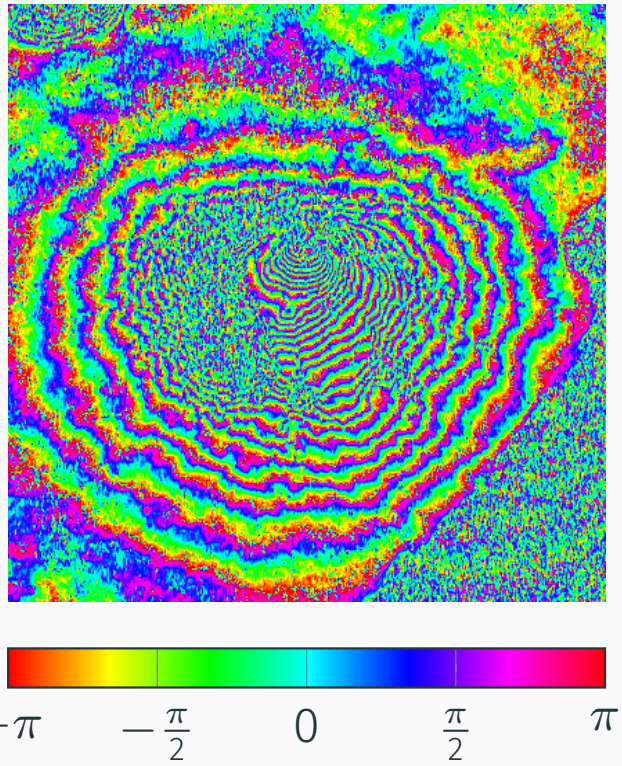

InSAR data of Mt. Vesuvius
[Rocca, Prati, Guarnieri '97]

$\mathbb{S}^1$

Manifold-valued image processing

New data aquisition modalities $\Rightarrow$ non-Euclidean range of data

- Interferrometric synthetic aperture radar (InSAR)
- **Surface normals**
- Diffusion tensors in magnetic resonance imaging (DT-MRI)
- Electron backscattered diffraction (EBSD)
- Directional data: wind, flow, GPS,...

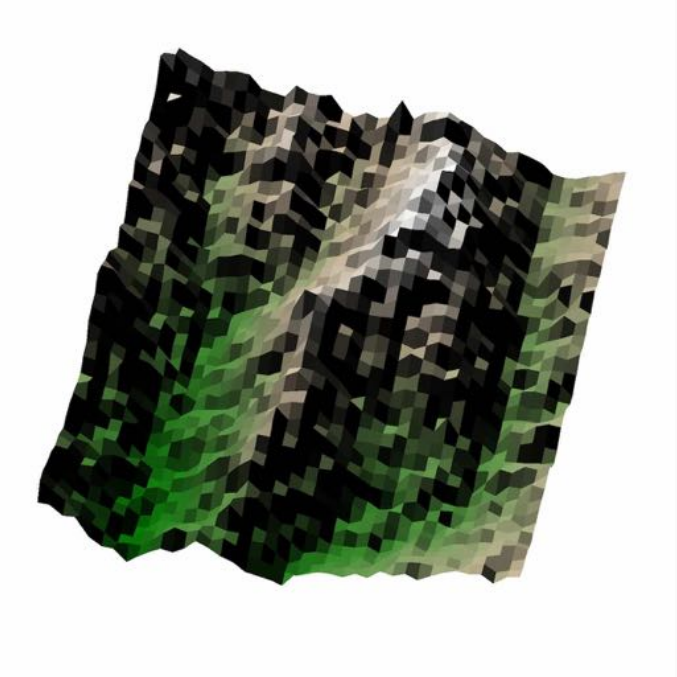

National elevation dataset
[Gesch, Evans, Mauck, '09; MFOPT/Lellmann]

$\mathbb{S}^2$

Manifold-valued image processing

New data aquisition modalities $\Rightarrow$ non-Euclidean range of data

- Interferrometric synthetic aperture radar (InSAR)
- Surface normals
- **Diffusion tensors in magnetic resonance imaging (DT-MRI)**
- Electron backscattered diffraction (EBSD)
- Directional data: wind, flow, GPS,...

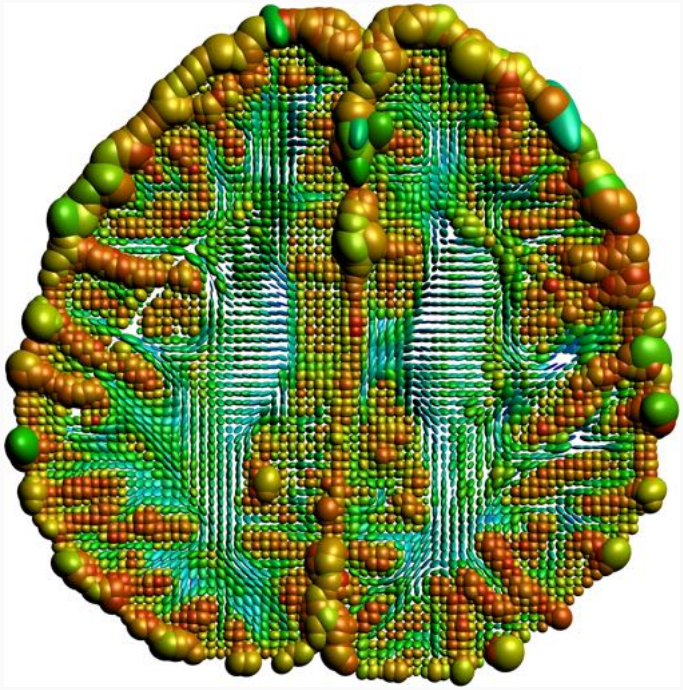

Slice # 28 from the Camino data set
http://cmic.cs.ucl.ac.uk/camino

3×3, sym. pos. def. matrices

Manifold-valued image processing

New data aquisition modalities $\Rightarrow$ non-Euclidean range of data

- Interferrometric synthetic aperture radar (InSAR)
- Surface normals
- Diffusion tensors in magnetic resonance imaging (DT-MRI)
- **Electron backscattered diffraction (EBSD)**
- Directional data: wind, flow, GPS,...

EBSD example from the MTEX toolbox
[Bachmann, Hielscher, since '05]

$\mathrm{SO}(3)$ (mod. symmetry)

Manifold-valued image processing

New data aquisition modalities $\Rightarrow$ non-Euclidean range of data

- Interferrometric synthetic aperture radar (InSAR)
- Surface normals
- Diffusion tensors in magnetic resonance imaging (DT-MRI)
- Electron backscattered diffraction (EBSD)
- Directional data: wind, flow, GPS,...

Similarities

- Range of the pixel is a Riemannian manifold
- Tasks of “classical” image processing

Variational methods

Goal. For given (lossy, noisy) measurements f reconstruct original data u_0 by minimizing the **Variational Model**

$$\mathcal{E}(u) := \underbrace{\mathcal{D}(u; f)}_{\text{data term}} + \underbrace{\alpha\, \mathcal{R}(u)}_{\text{regularization term}}, \qquad \alpha > 0.$$

Challenges

- reconstruction problem usually ill-posed/ill-conditioned
- high dimensional
- non-smooth but (hopefully) convex

Example. L^2-TV (ROF) model for a real valued signal $f \in \mathbb{R}^N$:

[Rudin, Osher, Fatemi, '92]

$$\operatorname*{arg\,min}_{u \in \mathbb{R}^N} \mathcal{E}(u) \;=\; \operatorname*{arg\,min}_{u \in \mathbb{R}^N} \|u - f\|^2 + \alpha \|\nabla u\|_1$$

Variational methods

Goal. For given (lossy, noisy) measurements f reconstruct original data u_0 by minimizing the **Variational Model**

$$\mathcal{E}(u) := \underbrace{\mathcal{D}(u; f)}_{\text{data term}} + \underbrace{\alpha\, \mathcal{R}(u)}_{\text{regularization term}}, \qquad \alpha > 0.$$

Challenges

- reconstruction problem usually ill-posed/ill-conditioned
- high dimensional
- non-smooth but (hopefully) convex

Example. L^2-TV (ROF) model for a real valued signal $f \in \mathbb{R}^N$:

[Rudin, Osher, Fatemi, '92]

$$\operatorname*{arg\,min}_{u \in \mathbb{R}^N} \mathcal{E}(u) = \operatorname*{arg\,min}_{u \in \mathbb{R}^N} \sum_{i=1}^{N} (u_i - f_i)^2 + \alpha \sum_{i=1}^{N-1} |u_{i+1} - u_i|$$

Notations on a Riemannian manifold $\mathcal{M}$

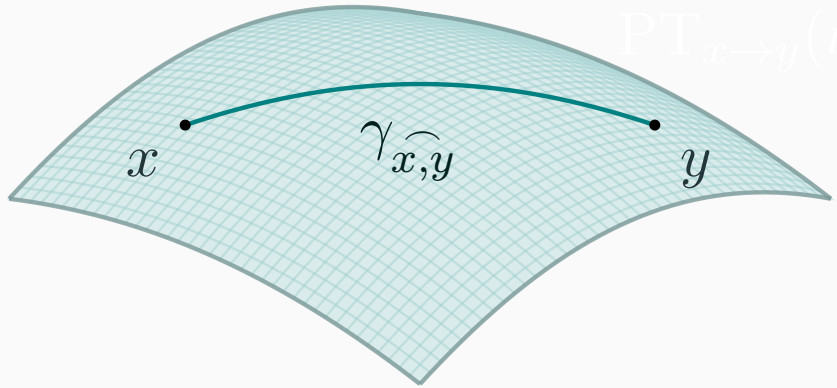

"A d-dimensional manifold can be informally defined as a set $\mathcal{M}$ covered with a 'suitable' collection of charts, that identify subsets of $\mathcal{M}$ with open subsets of $\mathbb{R}^d$."

[Absil, Mahony, Sepulchre, '08]

Notations on a Riemannian manifold $\mathcal{M}$

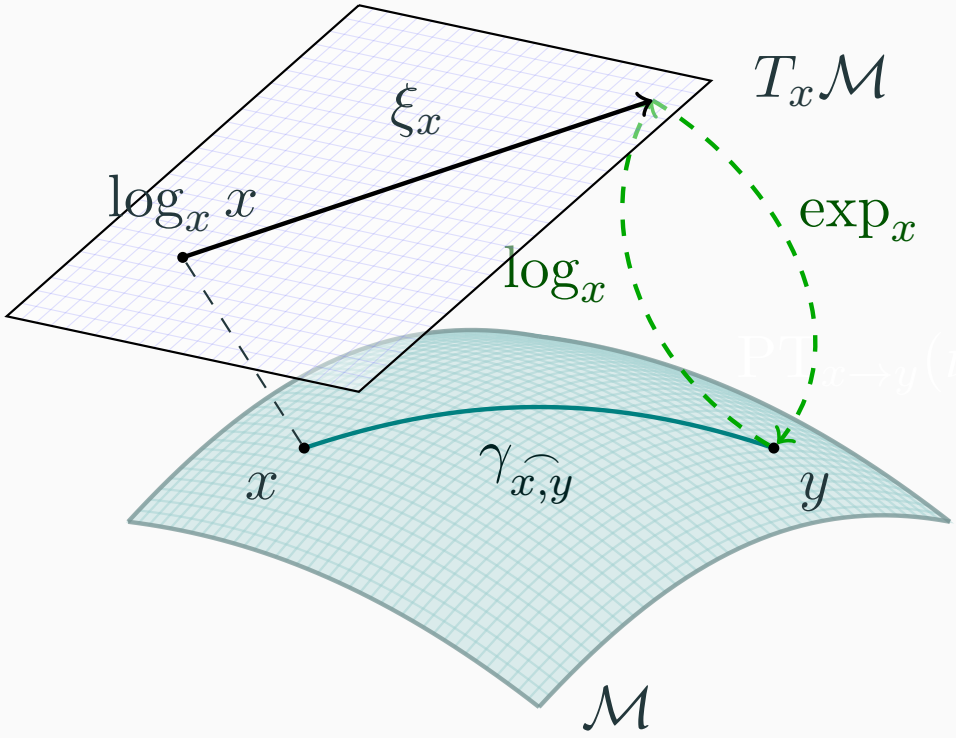

geodesic $\gamma_{\widehat{x,y}}$ shortest path (on $\mathcal{M}$) connecting $x, y \in \mathcal{M}$.
tangential plane $\mathrm{T}_x\mathcal{M}$ at x, $\mathrm{T}\mathcal{M} := \cup_{x\in\mathcal{M}}\mathrm{T}_x\mathcal{M}$
logarithmic map $\log_x y = \dot{\gamma}_{\widehat{x,y}}(0)$, "velocity towards y"
exponential map $\exp_x \xi_x = \gamma(1)$, where $\gamma(0) = x$, $\dot{\gamma}(0) = \xi_x$

First and Second Order Total Variation

- given data $f : \mathcal{V} \to \mathbb{R}$, $\mathcal{V} \subseteq \mathcal{G} = \{1, \dots, N\} \times \{1, \dots, M\}$
- reconstruct $u_0 : \mathcal{G} \to \mathbb{R}$, inpaint pixel from $\mathcal{G} \backslash \mathcal{V}$
- first order models (total variation, TV)

[Rudin, Osher, Fatemi, '92]

$$\mathcal{R}(u) = \mathrm{TV}(\mathrm{u}) = \sum_{i \in \mathcal{G}, j \in \mathcal{N}_i} \|u_i - u_j\|$$

- second order models (reduce staircasing):

[Chambolle, Lions, '97; Setzer, Steidl, '08; Bredies, Kunisch, Pock, '10; Papafitsoros, Schönlieb, '14]

For each $i \in \mathcal{G}$ with pre/successor $j, k \in \mathcal{G}$

$$\mathcal{R}(u) = \beta_1 \mathrm{TV}(u) + \beta_2 \sum_{i \in \mathcal{G}} d_2(u_j, u_i, u_k)$$

$$d_2(x, y, z) := \|x - 2y + z\|$$

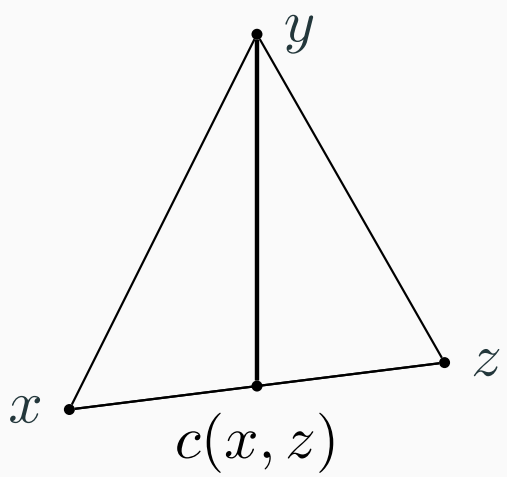

First and Second Order Total Variation

- given data $f : \mathcal{V} \to \mathcal{M}$, $\mathcal{V} \subseteq \mathcal{G} = \{1, \dots, N\} \times \{1, \dots, M\}$
- reconstruct $u_0 : \mathcal{G} \to \mathcal{M}$, inpaint pixel from $\mathcal{G} \backslash \mathcal{V}$
- first order models (total variation, TV)

[Weinmann, Storath, Demaret, '14, Lellmann, Koetters, Strekalovskij, Cremers, '13]

$$\mathcal{R}(u) = \mathrm{TV}(\mathrm{u}) = \sum_{i \in \mathcal{G}, j \in \mathcal{N}_i} d_{\mathcal{M}}(u_i, u_j)$$

- second order models (reduce staircasing):

  For each $i \in \mathcal{G}$ with pre/successor $j, k \in \mathcal{G}$

[Báčak, RB, Steidl, Weinmann, '16]

$$\mathcal{R}(u) = \beta_1 \, \mathrm{TV}(u) + \beta_2 \sum_{i \in \mathcal{G}} d_2(u_j, u_i, u_k)$$

$$d_2(x, y, z) := \min_{c \in \mathcal{C}_{x,z}} d_{\mathcal{M}}(c, y),$$

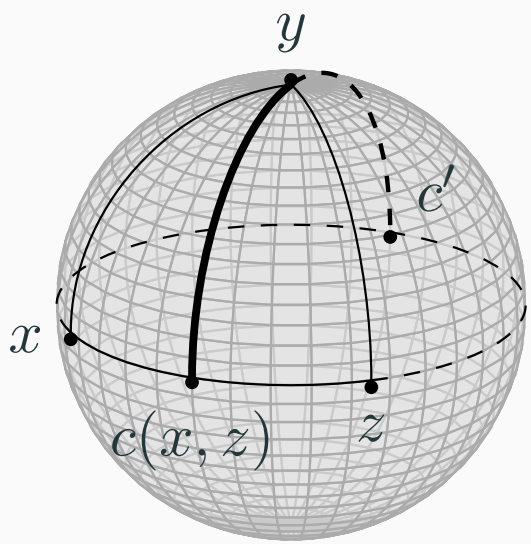

The Manifold-valued Image Restoration Toolbox

- inspired by Manopt[1]; focus on image processing
- implemented in Matlab & C++ (`mex`); Julia in process
- easy access to manifold-valued image processing

www.github.com/kellertuer/mvirt

- manifolds; object with `exp,log,dist,parallelTransport`
  - symmetric positive definite $d \times d$ matrices $\mathcal{P}(d)$
  - special orthogonal group $\mathrm{SO}(3)$
  - spheres $\mathbb{S}^n$
  - hyperbolic spaces $\mathcal{H}^n$
  - ...
- algorithms implemented on the abstract `manifold` object
- plot functions and exports to TikZ/Asymptote

[1] manopt.org - Optimization on Manifolds in Matlab

Algorithms within MVIRT

- **Proximal maps**

$$\operatorname{prox}_{\lambda\varphi}(g) := \operatorname*{arg\,min}_{u\in\mathcal{M}^n} \frac{1}{2}\sum_{i=1}^{n} d(u_i, g_i)^2 + \lambda\varphi(u).$$

  for

  - quadratic data term $\varphi(x) = d_{\mathcal{M}}(x, f)^2, \quad f \in \mathcal{M}$ [Ferrera, Oliveira, '02]
  - first order absolute differences $\varphi(x) = d_{\mathcal{M}}(x_1, x_2)$ [Weinmann, Storath, Demaret,'14]
  - second order absolute differences $\varphi(x) = d_2(x_1, x_2, x_3)$
    - analytical solution for $\mathbb{S}^1$ [RB, Laus, Steidl, Weinmann, '14]
    - numerical solution otherwise, [Bačák, RB, Steidl, Weinmann, '16]
      using a gradient descent, geodesic variation & Jacobi fields

- **Cyclic Proximal Point Algorithm** [Bertsekas, '11; Bačák, '14]

$$x^{(k+\frac{l+1}{c})} = \operatorname{prox}_{\lambda_k\varphi_l}(x^{(k+\frac{l}{c})}), \quad i = 0, \dots, c-1,\ k > 0$$

- **Nonlocal Minimum Mean-Square Estimator (NL-MSSE)** [Laus, Nikolova, Persch, Steidl, '17]
- **Median, Mean,...**

Algorithms soon within MVIRT

- **Half-Quadratic Minimzation** [RB, Chan, Hielscher, Persch, Steidl, '16]
  - c-transform (e.g. for $c(s,t) = t^2 s$)

    $$\varphi^c(s) := \inf_{t\in\mathbb{R}} \{c(t,s) - \varphi(t)\}.$$

    and employ the equality $\varphi^{cc} = \varphi$ for c-concave φ
  - Apply an alternating minimization (w.r.t. u and s)
    $\Rightarrow$ Quasi-Newton iteration
- **Douglas-Rachford splitting** [RB, Persch, Steidl, '16]
  Based on proximal maps & Reflections ($R_p(x) = 2p - x$):
  - $\mathcal{R}_p(x) = \exp_p(-\log_p(x))$
  - $\mathcal{R}_\varphi(x) = \mathcal{R}_{\mathrm{prox}_\varphi}(x)$
  - to minimize a sum of two functions $\varphi + \psi$:
    iterate $\mathcal{R}_{\eta\varphi} \circ \mathcal{R}_{\eta\psi}$ with a fixed step size reduction
- **graph p-Laplacian** [RB, Tenbrinck, '17]
  process data on surfaces,
  common framework for local and nonlocal methods

A signal of cyclic data

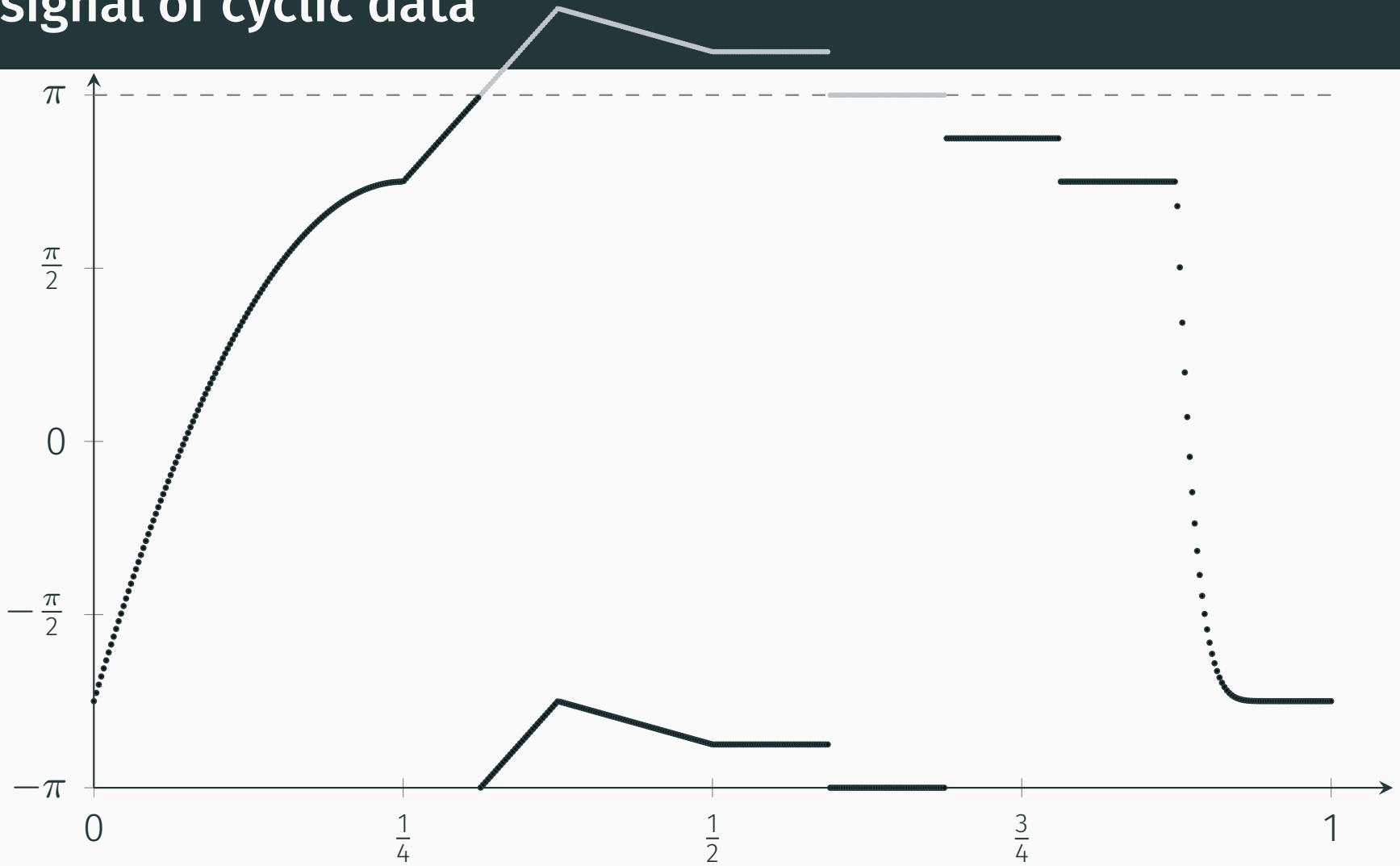

- Sample $f\colon [0,1] \to \mathbb{S}^1$ to obtain a signal $f_0 = (f_{0,i})_{i=1}^{500}$
- data f might stem from gray plot (modulo)
- Jumps $> \pi$ at $\frac{5}{16}$ and $\frac{11}{16}$ due to representation

A signal of cyclic data

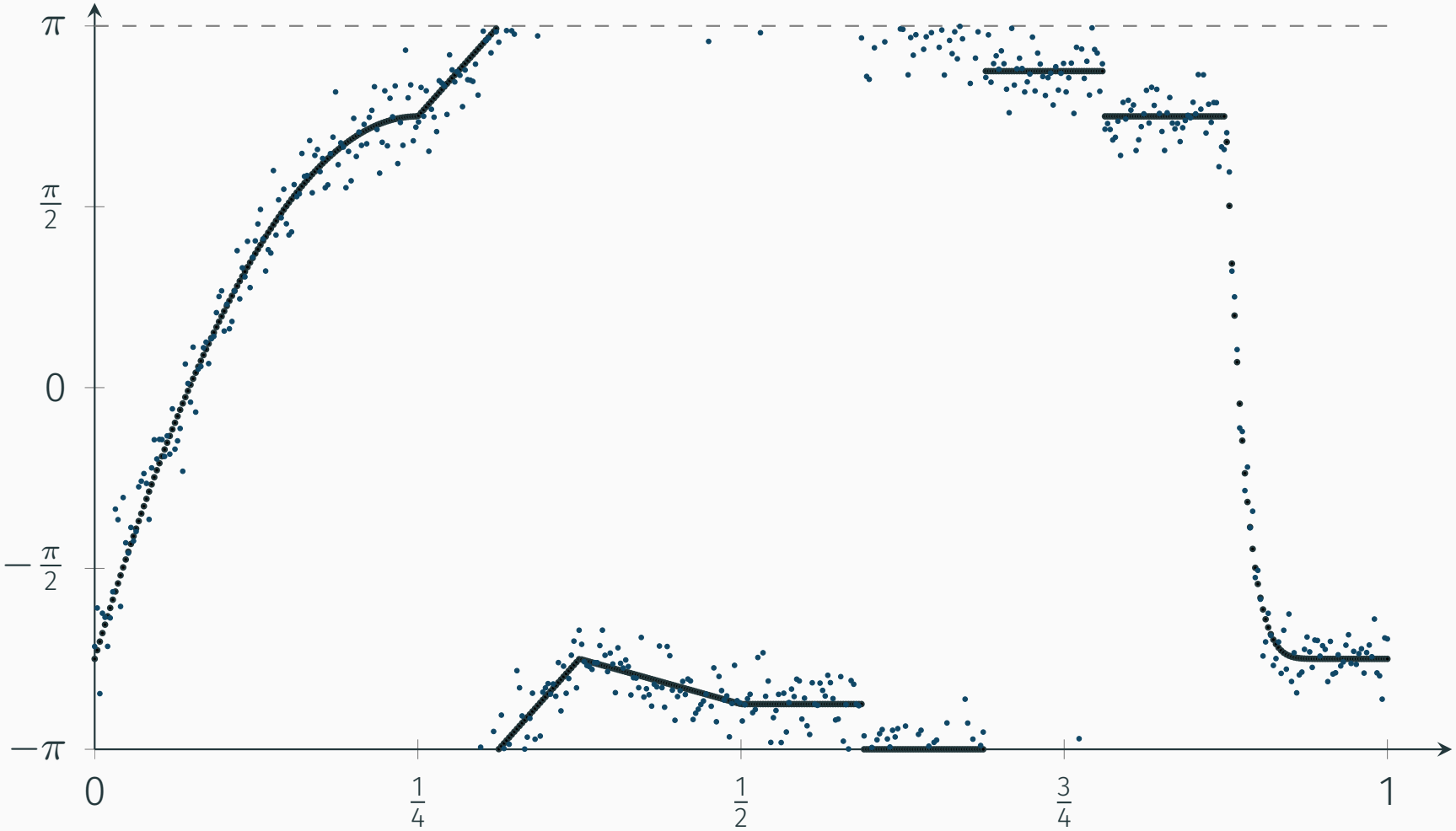

- Sample $f : [0, 1] \to \mathbb{S}^1$ to obtain a signal $f_{\mathrm{o}} = (f_{\mathrm{o},i})_{i=1}^{500}$
- Noise: wrapped Gaussian, $\sigma = 0.2$
- noisy $f_{\mathrm{n}} = (f_{\mathrm{o}} + \eta)_{2\pi}$

A signal of cyclic data

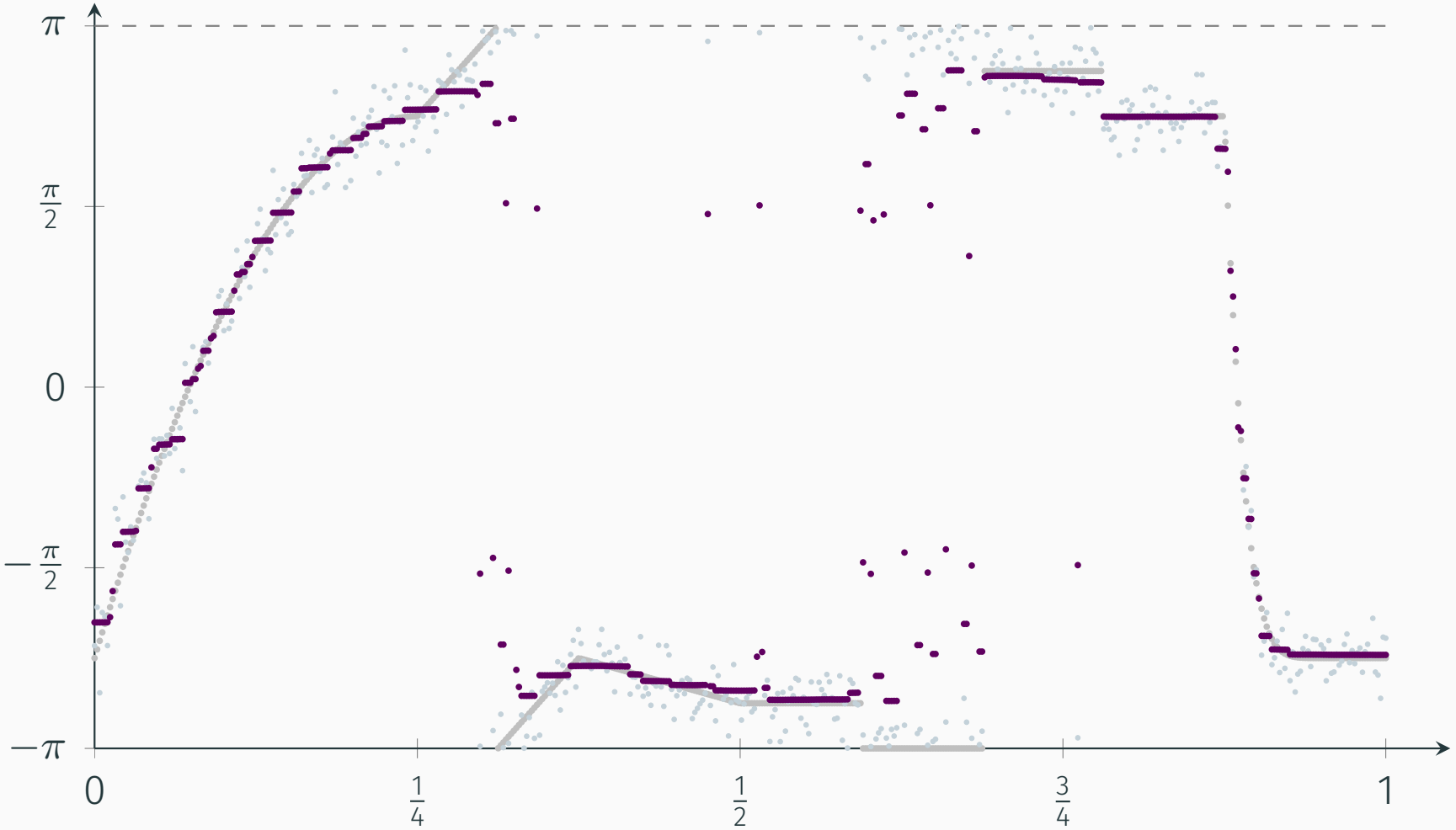

- Comparison of f_{o} & f_{n} with f_{R}
- Denoised with real-valued L^2-TV, ($\alpha = \frac{3}{4}$, $\beta = 0$)
- yields artefacts due to jumps stems from representation

A signal of cyclic data

- Comparison of f_0 & f_n with f_1
- Denoised with periodic L^2-TV_1 ($\alpha = \frac{3}{4}$, $\beta = 0$)
  [Strekalovskiy, Cremers '11]
- but: staircasing

A signal of cyclic data

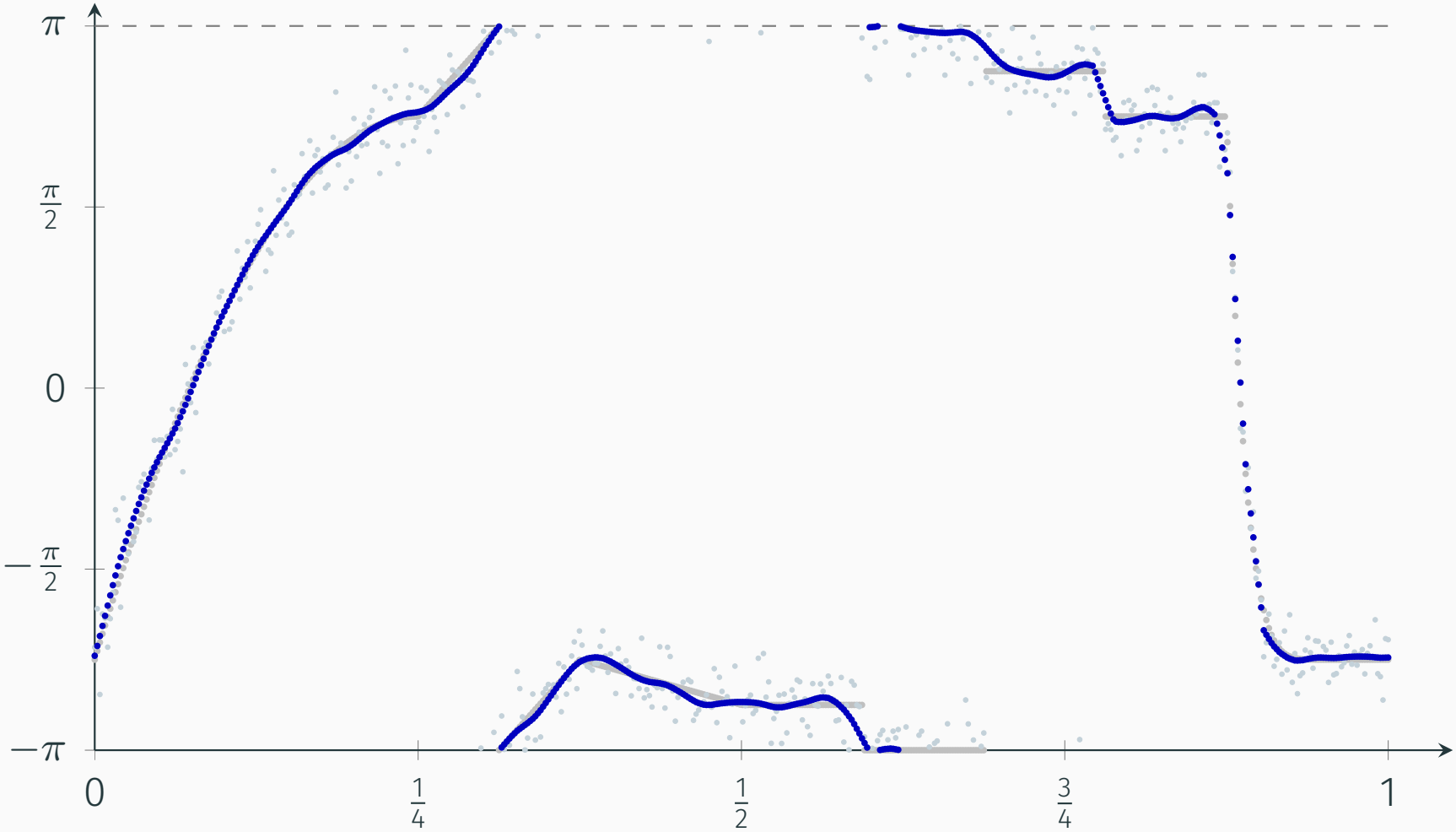

- Comparison of f_0 & f_n with f_2
- Denoised with periodic L^2-TV_2 ($\alpha = 0, \beta = \frac{3}{2}$)

[RB, Laus, Steidl, Weinmann '14]

- but: linear parts in constant areas

A signal of cyclic data

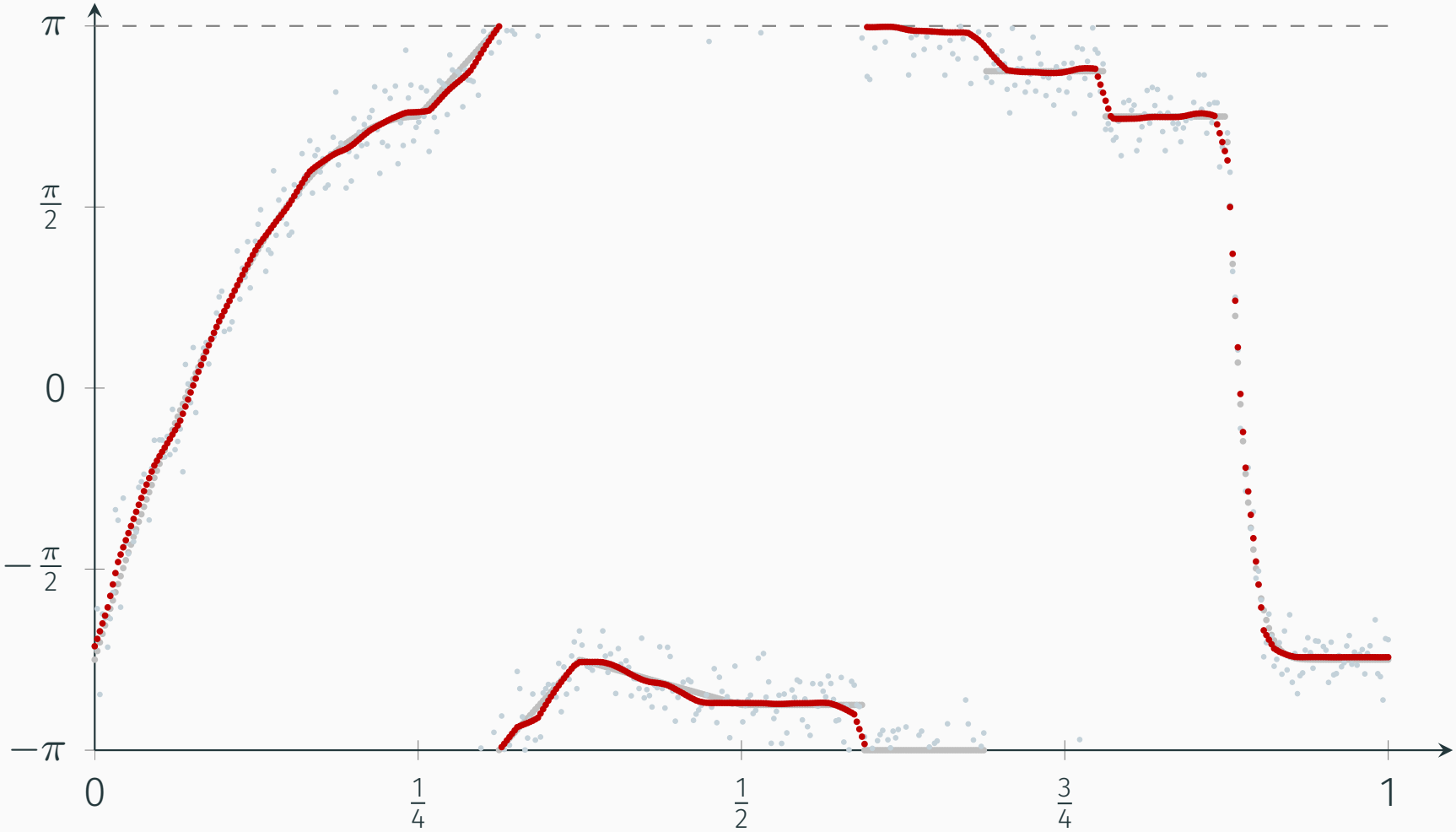

- Comparison of f_0 & f_n with f_3
- Denoised with periodic L^2-TV_1-TV_2 $(\alpha = \frac{1}{4}, \beta = \frac{3}{4})$

[RB, Laus, Steidl, Weinmann '14]

- combine both: smallest MSE.

An image of symmetric positive definite matrices

- Use L^2-TV on manifold-valued data of $\mathcal{P}(3)^{16\times16}$
- combined denoising and inpainting
- Douglas-Rachford algorithm for minimization

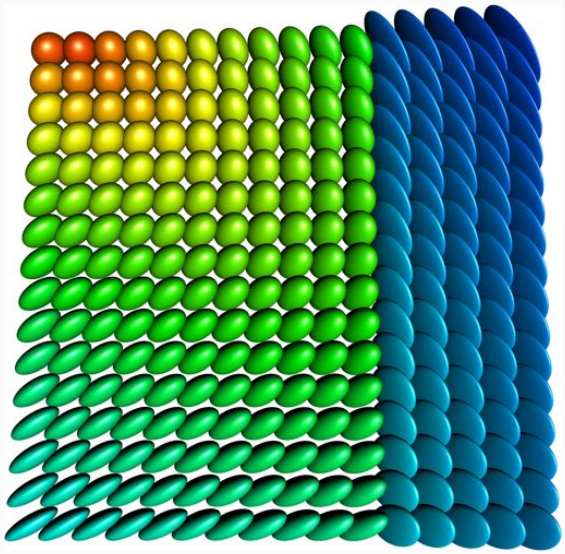

Original data

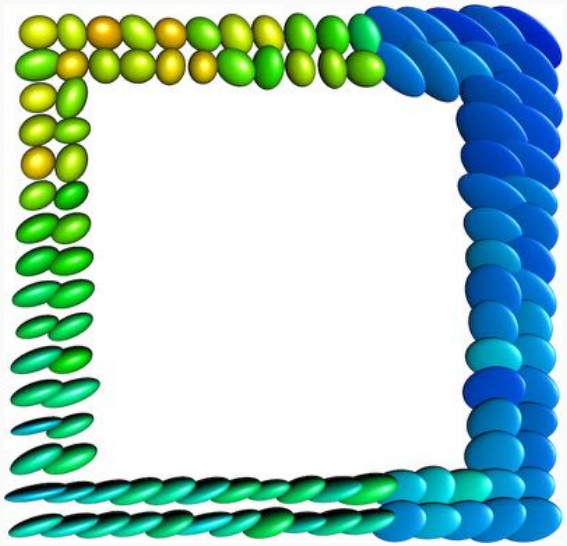

Lossy & noisy
Rician, $\sigma = 0.01$.

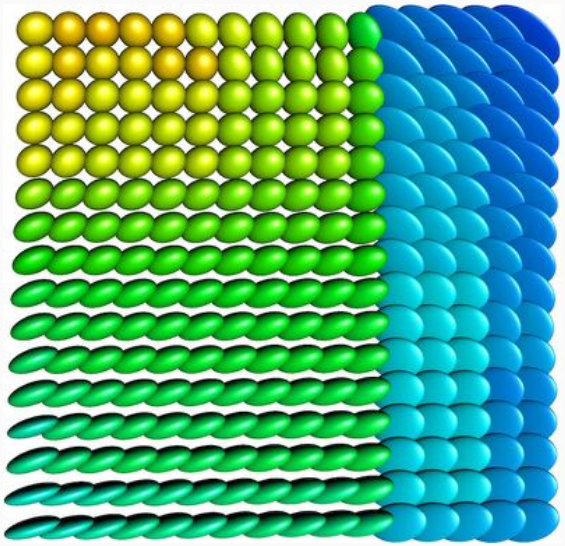

Reconstruction,
$\alpha = 0.01$

Diffusion tensor imaging

Given: Diffusion tensor volumetric data $\mathcal{P}(3)^{112\times112\times50}$ of the human head

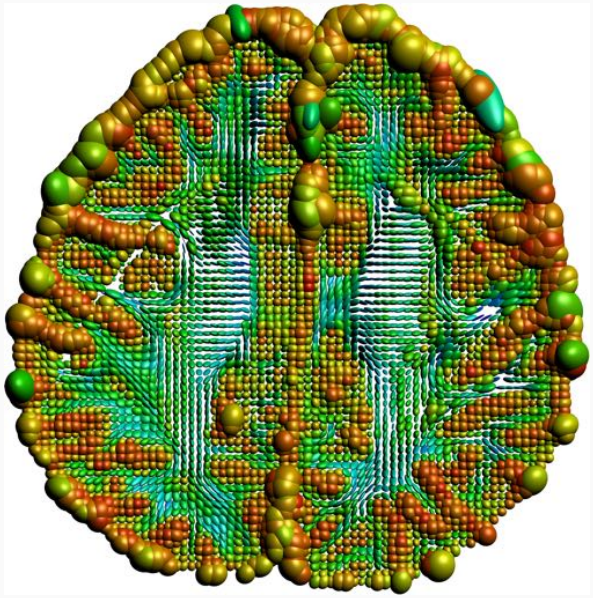

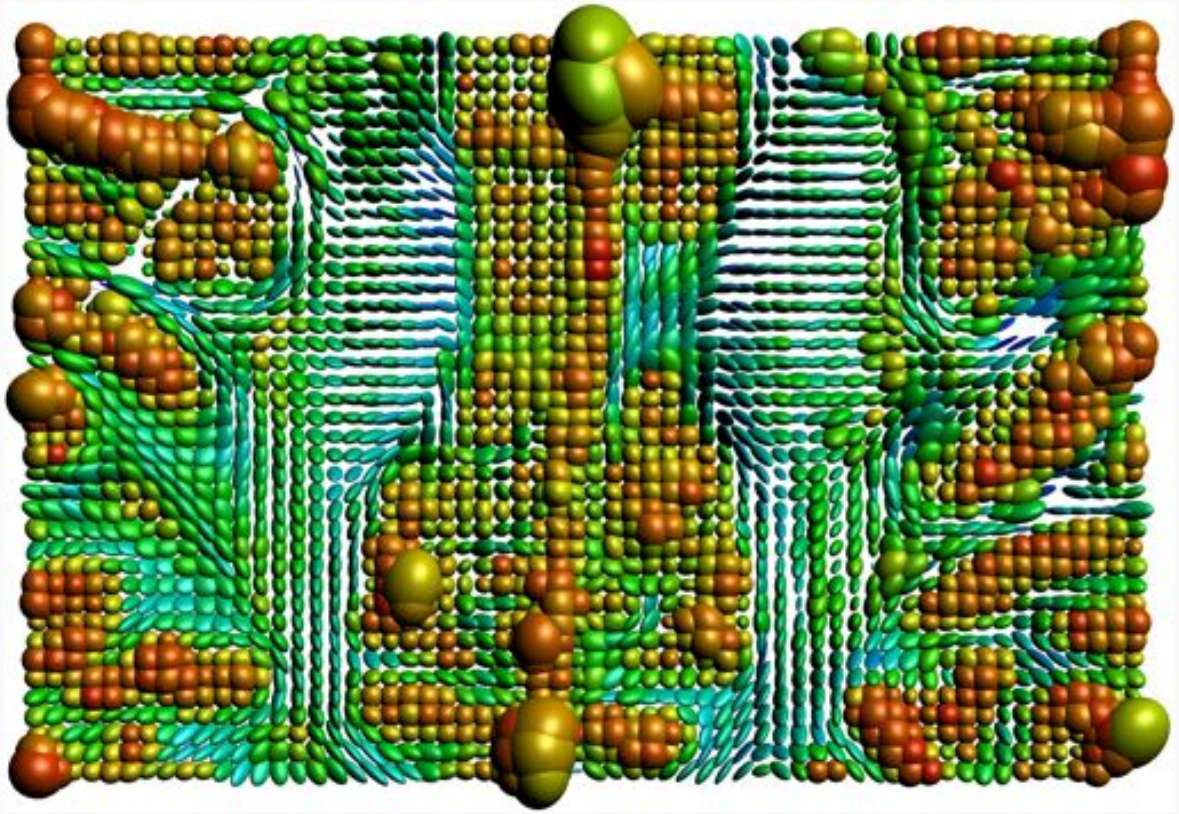

Original data, traversal plane $z = 28$.

(Data from the Camino project, cmic.cs.ucl.ac.uk/camino)

Diffusion tensor imaging

Given: Diffusion tensor volumetric data $\mathcal{P}(3)^{112\times112\times50}$ of the human head

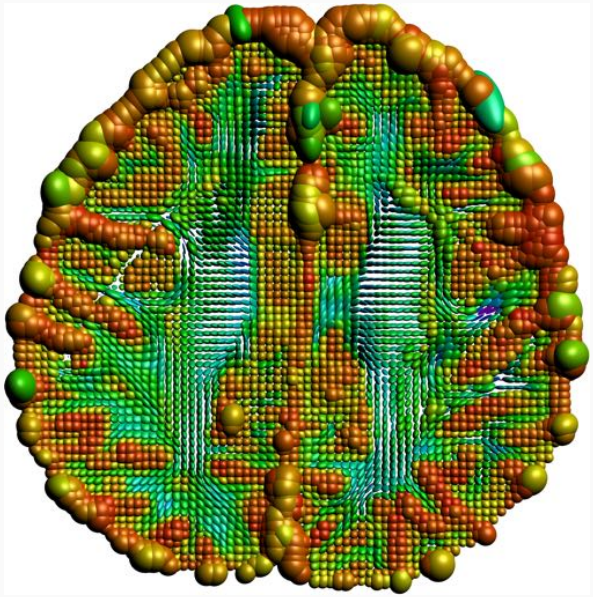

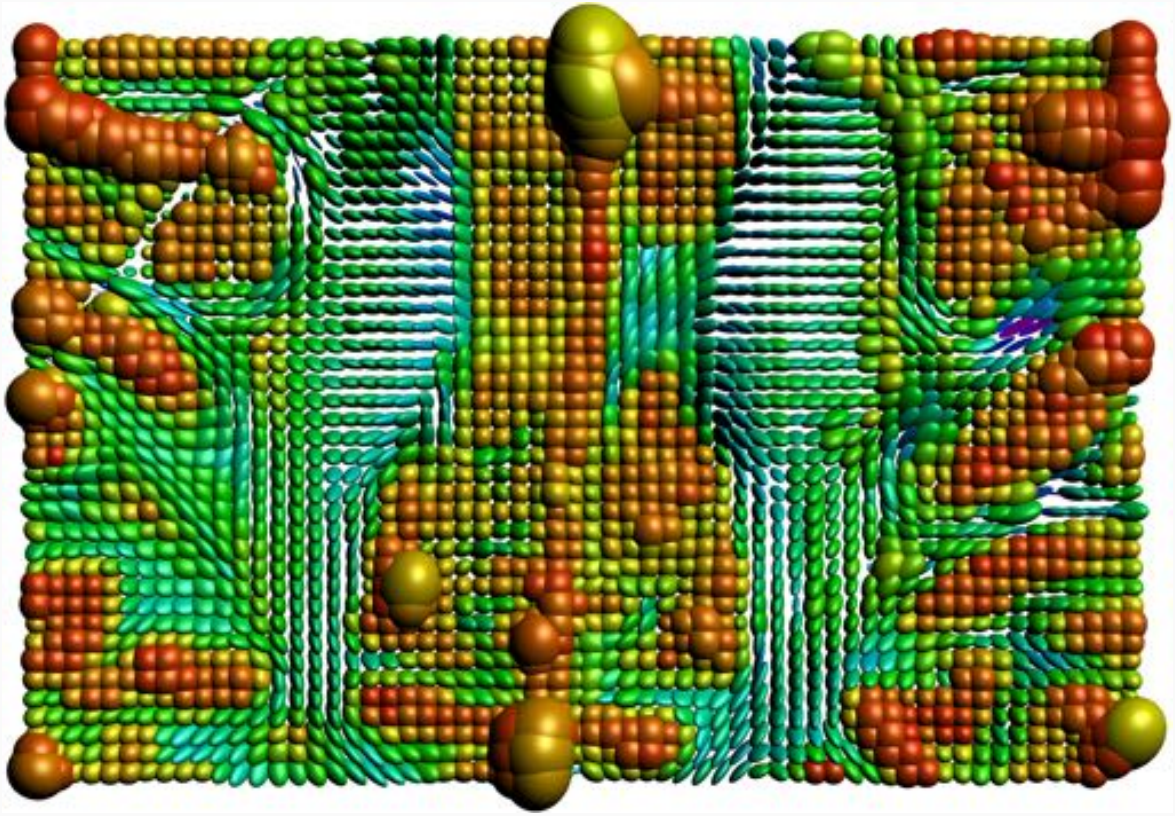

ROF modell, $\alpha = 0.1$

(Data from the Camino project, cmic.cs.ucl.ac.uk/camino)

Perspective: Denoising on an implicit surface

- $\mathcal{M} = \mathcal{P}(3)$, data at the nodes of a graphen $G = (V, E)$
- $V =$ point cloud: surface of the Camino data set
- $E =$ local neighbors in $\mathbb{R}^3$, $d_{\max} = 2$

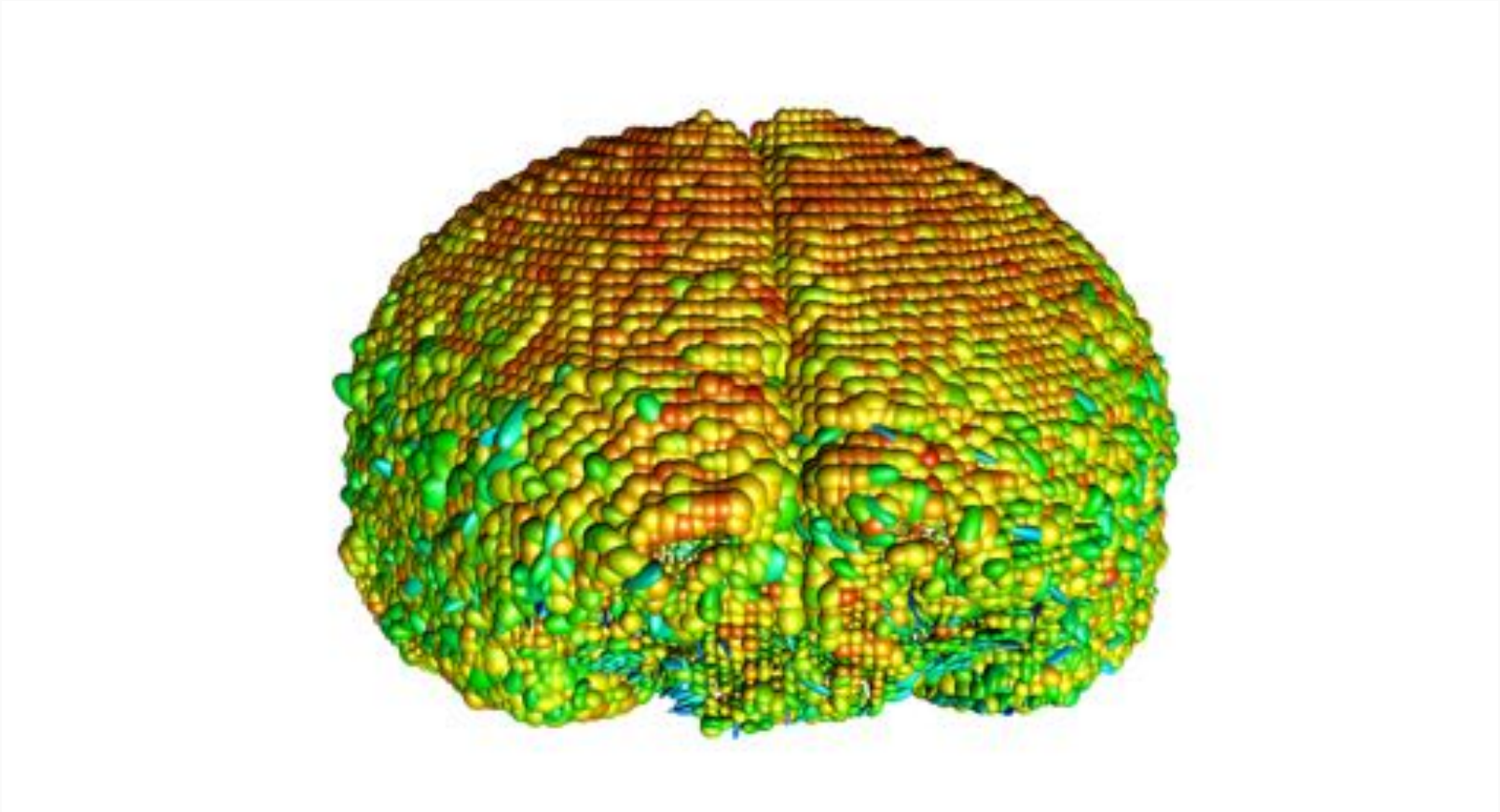

Original data

[RB, Tenbrinck, '17]

Perspective: Denoising on an implicit surface

- $\mathcal{M} = \mathcal{P}(3)$, data at the nodes of a graphen $G = (V, E)$
- $V =$ point cloud: surface of the Camino data set
- $E =$ local neighbors in $\mathbb{R}^3$, $d_{\max} = 2$

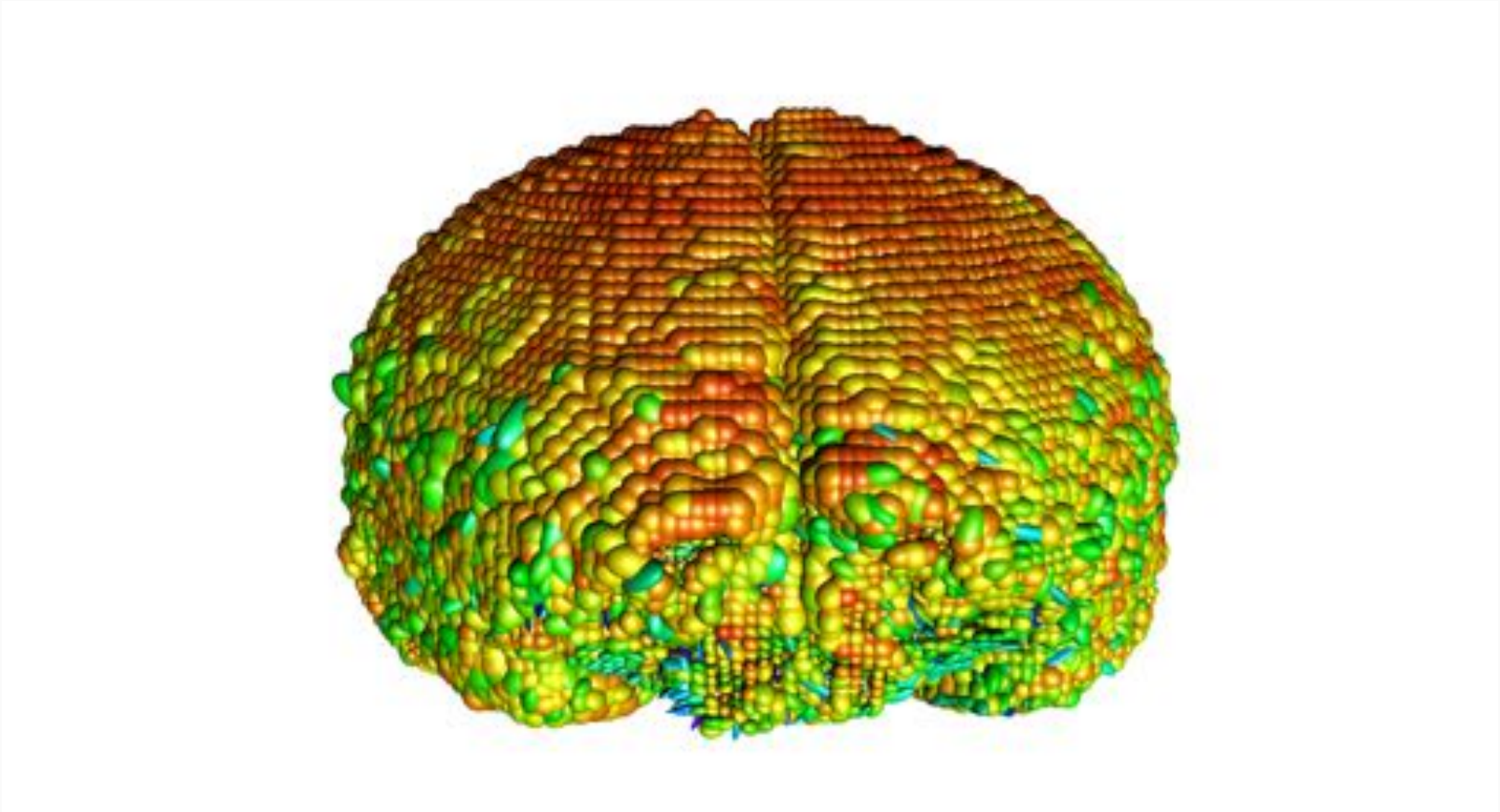

$\lambda = 50$, anisotropic graph-1-Laplace; TV on the surface.

[RB, Tenbrinck, '17]

Literature


RB und D. Tenbrinck. A graph framework for manifold-valued data. 2017. arXiv: 1702.05293.


RB, J. Persch und G. Steidl. “A parallel Douglas-Rachford algorithm for restoring images with values in symmetric Hadamard manifolds”. In: SIAM J. Imaging Sci. 9.4 (2016), S. 901–937.


RB, R. H. Chan, R. Hielscher, J. Persch und G. Steidl. “Restoration of Manifold-Valued Images by Half-Quadratic Minimization”. In: Inv. Probl. Imag. 2.10 (2016), S. 281–304.


M. Bačák, RB, G. Steidl und A. Weinmann. “A second order non-smooth variational model for restoring manifold-valued images”. In: SIAM J. Sci. Comput. 38.1 (2016), A567–A597.


RB und A. Weinmann. “A second order TV-type approach for inpainting and denoising higher dimensional combined cyclic and vector space data”. In: J. Math. Imaging Vision 55.3 (2016), S. 401–427.


RB, F. Laus, G. Steidl und A. Weinmann. “Second order differences of cyclic data and applications in variational denoising”. In: SIAM J. Imaging Sci. 7 (4 2014), S. 2916–2953.